Journal of Theoretical Biology 293 (2012) 197–205

Contents lists available at SciVerse ScienceDirect

Journal of Theoretical Biology

journal homepage: www.elsevier.com/locate/yjtbi

Elastic and viscoelastic properties of a type I collagen fiber

Ratchada Sopakayang [a,1], Raffaella De Vita [b,*], Albert Kwansa [b], Joseph W. Freeman [c]

[a] Department of Mechanical Engineering, Faculty of Engineering, Ubon Ratchathani University, Warinchumrap, Ubon Ratchathani 34190, Thailand
[b] Mechanics of Soft Biological Systems Laboratory, Engineering Science and Mechanics Department, 202 Norris Hall, Virginia Tech, Blacksburg, 24061 VA, United States
[c] Musculoskeletal Tissue Regeneration Laboratory, 599 Taylor Road, Piscataway, 08854 NJ, United States

ARTICLE INFO

Article history:
Received 17 January 2011
Received in revised form
14 September 2011
Accepted 14 October 2011
Available online 21 October 2011

Keywords:
Viscoelastic model
Structural model
Incremental stress relaxation
Collagen fiber
Rat tail tendons

ABSTRACT

A new mathematical model is presented to describe the elastic and viscoelastic properties of a single collagen fiber. The model is formulated by accounting for the mechanical contribution of the collagen fiber's main constituents: the microfibrils, the interfibrillar matrix and crosslinks. The collagen fiber is modeled as a linear elastic spring, which represents the mechanical contribution of the microfibrils, and an arrangement in parallel of elastic springs and viscous dashpots, which represent the mechanical contributions of the crosslinks and interfibrillar matrix, respectively. The linear elastic spring and the arrangement in parallel of elastic springs and viscous dashpots are then connected in series. The crosslinks are assumed to gradually break under strain and, consequently, the interfibrillar is assumed to change its viscous properties. Incremental stress relaxation tests are conducted on dry collagen fibers reconstituted from rat tail tendons to determine their elastic and viscoelastic properties. The elastic and total stress–strain curves and the stress relaxation at different levels of strain collected by performing these tests are then used to estimate the parameters of the model and evaluate its predictive capabilities.

1. Introduction

The mechanical behavior of collagenous tissues such as ligaments and tendons is mainly determined by their constituent collagen fibers. The collagen fibers are indeed considered to be the main load bearing components of these tissues. Each collagen fiber is composed of numerous collagen fibrils that are usually aligned along one direction. The collagen fibrils are, in turn, made of microfibrils that are composed of five strands of collagen molecules, which are staggered along the axial microfibril direction (Silver et al., 2003). The microfibrils in a collagen fibril are stabilized by covalent crosslinks and are embedded in a proteoglycan-rich matrix (Raspanti et al., 2002). Crosslinks are deemed responsible for stabilizing and reinforcing a single collagen fiber (Robins, 1982; Davison and Brennan, 1983). As a tissue develops and matures, native crosslinks increase in functionality as they form more stable, mature crosslinks between collagen molecules and microfibrils (Couppe et al., 2009).

The types of crosslinks in ligaments and tendons have been fairly well characterized, primarily by high-performance liquid chromatography methods, but the locations and mechanisms of crosslink maturation are not completely understood (Sims and Bailey, 1992; Saito et al., 1997; Eyre and Wu, 2005; Avery and Bailey, 2008). The increase in crosslinks influences the mechanical properties of collagen fibers, ligaments and tendons by producing, for example, an increase in their corresponding stiffness (Puxkandl et al., 2002; Hansen et al., 2009).

Puxkandl et al. (2002) studied the effect of crosslinks by performing tensile tests and synchrotron X-ray scattering on normal and crosslink-deficient rat tail tendons. In their study, the ultimate load and stiffness were significantly higher in normal rat tail tendons than in crosslink-deficient rat tail tendons, but the ultimate deformation for these two groups of tendons was not significantly different. These results suggested that the crosslinks do not alter the deformation of the tendons. The tendons were also modeled as a series of two different Kelvin–Voigt elements: the first one represented the contribution of collagen fibrils and their crosslinks and the second one represented the contribution of the proteoglycan-rich matrix. In the first Kelvin–Voigt element, the elastic modulus of the spring was assumed to depend on the density of the crosslinks in the fibrils while the viscosity of the dashpot was assumed to be due to the friction between the collagen molecules in fibrils. The model was shown to fit well tensile data of normal and crosslink-deficient rat tail tendons but was not compared to the experimental data at the fibril (or fiber) level.

Hansen et al. (2009) performed tensile tests on fibrils by using atomic force microscopy and on fascicles by employing

* Corresponding author. Tel.: +1 540 231 5905.
E-mail address: devita@vt.edu (R. De Vita).
[1] The authors are listed in the order of importance of their individual contributions to the work.

0022-5193/$ - see front matter © 2011 Elsevier Ltd. All rights reserved.
doi:10.1016/j.jtbi.2011.10.018

a custom-built tensile testing device. The fibers and fascicles were excised from normal and chemically treated rat tail tendons. The chemical treatment was used to induce crosslinks in the tendons. The authors found that the elastic modulus was considerably higher for fibrils but only slightly higher for fascicles when extracted from chemically treated rat tail tendons. Thus, they concluded that the strength of the whole tissue depends mainly on the crosslinks that are present at the collagen fibril level.

Recently, Gupta et al. (2010) employed high time resolution synchrotron X-ray diffraction and confocal microscopy to investigate stress relaxation both at the fibril and fiber levels in rat tail tendons. In order to interpret the results of the experiments, the authors proposed a viscoelastic model, which consisted of an arrangement in series of a Kelvin–Voigt element and two different Maxwell elements. The Kelvin–Voigt element represented the collagen fibrils with their crosslinks, one Maxwell element represented the interfibril proteoglycan-rich matrix while the other Maxwell element represented the inter-fiber ground substance. The model fitted well stress relaxation data at both fibril and fiber levels. These results indicated that the mechanisms governing stress relaxation at the fibril and fiber length scales are different and are affected by the presence of crosslinks.

Incremental stress relaxation tests have been used by Silver and his colleagues to elucidate the structural mechanisms most likely contributing to the viscoelastic behaviors in collagenous tissues and in fibril-forming collagens such as collagen type I (Silver et al., 2001a, 2001b, 2002). Unlike tensile and stress relaxation tests, incremental stress relaxation tests provide valuable information on the elastic and viscoelastic properties of collagenous tissues. During an incremental stress relaxation test, a specimen is pulled at a fixed strain rate to some relative level of incremental strain (i.e., 5%). Thereafter, the specimen is held at that fixed strain until the stress decays to an equilibrium or residual stress. Then an additional incremental strain is placed upon the specimen, and the stress is again allowed to decay to an equilibrium value. These incremental strain and stress relaxation cycles are repeated until the specimen fails (Silver et al., 2000). During the analysis of incremental stress relaxation data, stress and strain values can be obtained for each incremental strain value (i.e., 5%, 10%, 15%). The stress before relaxation is often called the total or initial stress, while the stress after relaxation is commonly termed the elastic or equilibrium/residual stress, and the difference between the total and elastic stresses is the viscous stress. Total, elastic, and viscous stresses can be plotted against strain to produce incremental stress–strain plots.

In this study, a new mathematical model for individual collagen fibers is formulated by considering their structure and composition including the microfibrils, crosslinks and interfibrillar matrix. The novelty of the model is determined by its ability to describe both the elastic and viscoelastic properties of the collagen fibers as determined by incremental stress relaxation tests. As indicated by previous experimental studies (Puxkandl et al., 2002; Hansen et al., 2009; Gupta et al., 2010) the microfibrils, crosslinks and interfibrillar matrix are responsible for the elasticity and viscoelasticity of collagenous fibers. In the model, the collagen fiber is assumed to consist of an arrangement in series of a linear elastic spring, which represents the mechanical contribution of the microfibrils, with an arrangement in parallel of elastic springs and viscous dashpots, which represent the mechanical contributions of the crosslinks and interfibrillar matrix. The crosslinks are assumed to gradually break under strain and, consequently, the interfibrillar matrix is assumed to change its viscous properties. Incremental stress relaxation tests are conducted on dry collagen fibers reconstituted from rat tail tendons to determine their elastic and viscoelastic properties. The elastic and total stress–strain curves and the stress relaxation at different levels of strain are then used to estimate the parameters of the model and evaluate its predictive capabilities. To the authors' knowledge, this is the first attempt to model the elastic and viscoelastic behavior of individual collagen fibers determined from incremental stress relaxation tests by accounting for their micro-structure.

2. Materials and methods

2.1. Extraction and purification of collagen type I

Tail tendons were obtained from Sprague-Dawley rats in accordance with an approved Virginia Tech IACUC protocol. The rat tails were received from other research groups either through lab-to-lab transfer or through Virginia Tech's Central Vivarium. In both cases, all rats had already been euthanized and the rat tails would have otherwise been discarded. Acid-soluble collagen protein was extracted and purified from rat tail tendons using a procedure described by Pins et al. (1997). Briefly, rat tail tendons were removed and partially dissolved in 10 mM hydrochloric acid (HCl, pH 2.0). The acid-soluble fraction was sterile-filtered ($0.8 \rightarrow 0.65 \rightarrow 0.45\ \mu m$), and the collagen was precipitated out using 0.7 M sodium chloride (NaCl); under acidic conditions, this concentration of NaCl has been shown to precipitate collagen types I–IV (Deyl and Adam, 1989). The collagen protein was collected via centrifugation and re-dissolved in 10 mM HCl, followed by dialysis against 20 mM sodium phosphate dibasic (pH 7.4). Lastly, the collagen was collected and re-dissolved as before, dialyzed against 10 mM HCl, and diluted to 10 mg/mL (checked by weighing the dry mass of collagen protein that remained after drying out the collagen solution in an oven at 110 °C).

2.2. Extruding reconstituted collagen fibers

Fourteen reconstituted collagen fibers were formed using a method described by Pins et al. (1997). Briefly, 10 mg/mL of collagen solution and fiber formation buffer (FFB) [135 mM sodium chloride (NaCl), 5 mM sodium phosphate dibasic (Na_2HPO_4), 30 mM tris hydroxymethyl aminomethane (THAM)] were separately loaded into a dual syringe system. The dual syringe pump was run at 0.7 mL/min, and the resulting mixture was extruded through 1 mm (I.D.) polytetrafluoroethylene (PTFE) tubing into a bath of FFB at ~35 °C. The bath temperature was controlled with an immersion heater (Cole Parmer, EW-03046-40). The fibers were kept in FFB at ~35 °C for 24 h, after which the FFB was replaced with fiber incubation buffer (FIB) [135 mM NaCl, 30 mM Na_2HPO_4, 10 mM THAM] (~35 °C, 24 h). The FIB was replaced with deionized water (~35 °C, 1 h), followed by replacement with fresh deionized water at room temperature. Then the fibers were removed and air-dried under slight tension. In order to ease handling, the fibers were affixed into vellum paper support frames with epoxy glue. The fibers were then physically aged in a Petri dish at room temperature (~23 °C) for 2 months before mechanical characterization. A scanning electron microscopy image of a fiber reconstituted from rat tail tendon collagen is shown in Fig. 1.

2.3. Mechanical testing

Prior to mechanical testing, the diameters of the fibers (assuming circular cross-sections) were measured at three locations per fiber using a Leica DM IL inverted light microscope equipped with a calibrated measurement scale. Fiber specimens were tested in air at ambient temperature (23.14 ∓ 0.20 °C) and

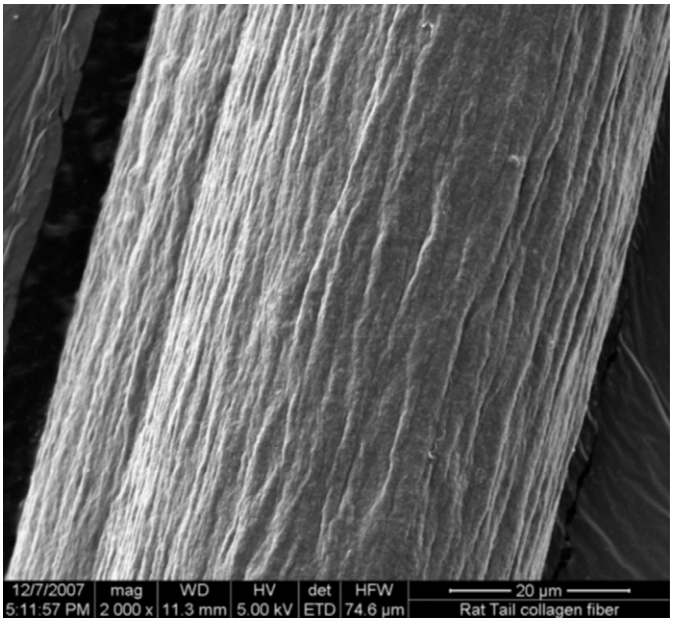

Fig. 1. SEM image of a reconstituted collagen fiber from rat tail tendons showing their fibrils.

ambient humidity ($40.13 \mp 11.88\%$RH) using an MTS Tytron 250 Microforce Testing System equipped with a ± 5 N load cell and a linear variable differential transformer (LVDT) to track specimen elongation. Incremental stress relaxation tests involved alternating pull and hold cycles repeated six times (each fiber was pulled to 2.5% relative strain at a rate of 10%/min and then held at a fixed strain for a pre-programmed length of time that changed with the level of overall strain). The pre-programmed hold times were as follows: 2.5% (30 min), 5% (1.5 h), 7.5% (2.5 h), 10% (3.5 h), 12.5% (4.5 h), and 15% (5.5 h).

3. Model formulation

3.1. Preliminaries

In formulating the model, an individual collagen fiber is assumed to consist of a linear elastic spring with elastic constant E_m and a series of linear elastic springs with elastic constants E_l and viscous dashpots with viscous constants η_m, which are arranged in series as shown in Fig. 2. The linear elastic spring with elastic constant E_m represents the total contribution of the microfibrils while the linear elastic springs with elastic constants E_l represent the contributions of the crosslinks existing among microfibrils, which gradually break under strain. The viscous dashpots with viscous constants η_m represent the contribution of the interfibrillar matrix. Because the crosslinks among microfibrils break under strain, the interaction between the microfibrils and the interfibrillar matrix is assumed to be altered under strain. Specifically, the viscous constant of the interfibrillar matrix, η_m, is equal to η_{m_u} for the crosslinks that are unbroken and is equal to η_{m_b} for the crosslinks that are broken.

3.2. General framework

A schematic of the model is presented in Fig. 2. As shown in Fig. 2, the total stress of a collagen fiber, $\sigma(t)$, is given by

$$\sigma(t) = \sigma_{E_m}(t) = \sigma_{E_l}(t) + \sigma_{\eta_m}(t), \tag{1}$$

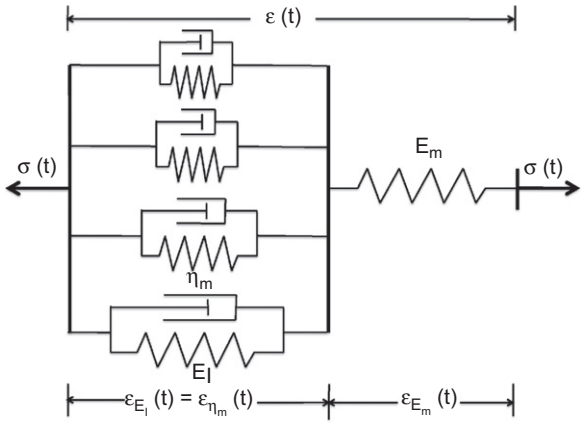

Fig. 2. Schematic of the viscoelastic model.

where $\sigma_{E_m}(t)$, $\sigma_{E_l}(t)$ and $\sigma_{\eta_m}(t)$ are the stresses of the microfibrils, crosslinks and interfibrillar matrix, respectively. Thus, according to Eq. (1) the contributions of the crosslinks and interfibrillar matrix to the total stress of a collagen fiber are different.

The total strain of a collagen fiber, $\varepsilon(t)$, is

$$\varepsilon(t) = \varepsilon_{E_m}(t) + \varepsilon_{E_l}(t) = \varepsilon_{E_m}(t) + \varepsilon_{\eta_m}(t), \tag{2}$$

where $\varepsilon_{E_m}(t)$, $\varepsilon_{E_l}(t)$ and $\varepsilon_{\eta_m}(t)$ are the strains of the microfibrils, crosslinks and interfibrillar matrix, respectively. It follows from Eq. (2) that $\varepsilon_{E_l}(t) = \varepsilon_{\eta_m}(t)$ that is the crosslinks and the interfibrillar matrix are subjected to the same strain.

The stress of the microfibrils is defined as

$$\sigma_{E_m}(t) = E_m \varepsilon_{E_m}(t), \tag{3}$$

where E_m denotes the elastic constant of the microfibrils. It must be emphasized that $\sigma_{E_m}(t)$, $\varepsilon_{E_m}(t)$ and E_m represent the stress, strain and elastic modulus, respectively, of all the microfibrils forming the collagen fiber.

The stress determined by the crosslinks in the collagen fiber is defined by using an approach similar to the one presented by Raischel et al. (2006) and De Tommasi et al. (2006) for different materials. The crosslinks are assumed to break when their strains ε_{E_l} reach some values $\varepsilon_b \geq 0$ that are defined by an exponential probability density function. Specifically, the stress of the crosslinks is given by

$$\sigma_{E_l}(t) = E_l \varepsilon_{E_l}(t)(1 - P(\varepsilon_{E_l}(t))) + E_l \int_0^{\varepsilon_{E_l}(t)} \varepsilon_b p(\varepsilon_b)\, d\varepsilon_b, \tag{4}$$

where E_l is the elastic constant of the crosslinks. In Eq. (4), $p(\varepsilon_b)$ is the probability density function associated with the event of a crosslink breaking at the strain $\varepsilon_b \geq 0$ and is assumed to be an exponential probability density function with rate α:

$$p(\varepsilon_b) = \alpha e^{-\alpha \varepsilon_b}, \tag{5}$$

where $\alpha > 0$ denotes the so-called rate parameter. Moreover, in Eq. (4), $P(\varepsilon_{E_l})$ denotes the exponential cumulative distribution function defined as

$$P(\varepsilon_{E_l}) = \int_0^{\varepsilon_{E_l}} p(\varepsilon_b)\, d\varepsilon_b = 1 - e^{-\alpha \varepsilon_{E_l}}, \tag{6}$$

which represents the density of broken crosslinks. Note that the rate parameter α admits an interpretation as the inverse of the characteristic strain at which most crosslinks break. The first term on the right-hand side of Eq. (4) is the stress of all the unbroken crosslinks while the second term is the stress of all the broken crosslinks. The stress of the broken crosslinks is not transferred to the unbroken crosslinks.

The stress of the interfibrillar matrix, $\sigma_{\eta_m}(t)$, is defined by taking into account the difference in the viscous constants determined by the breakage of crosslinks. Thus, the stress of the interfibrillar matrix is defined as

$$\sigma_{\eta_m}(t)=\eta_{m_u}\varepsilon'_{\eta_m}(t)(1-P(\varepsilon_{\eta_m(t)}))+\eta_{m_b}\varepsilon'_{\eta_m}(t)P(\varepsilon_{\eta_m(t)}), \tag{7}$$

where η_{m_u} and η_{m_b} denote the viscous constants of the interfibrillar matrix associated with the unbroken or broken crosslinks, respectively, and the prime denotes the differentiation with respect to t. In Eq. (7), the first term on the right hand side represents the contribution of the interfibrillar matrix with unbroken crosslinks while the second term represents the contribution of the interfibrillar matrix with broken crosslinks. It is assumed that the portion of the interfibrillar matrix with unbroken crosslinks and the remaining portion of the interfibrillar matrix with broken crosslinks are subjected to the same strain, $\varepsilon_{\eta_m}(t)$.

From Eqs. (3), (4), (7) it follows that Eq. (1) can be rewritten as

$$\begin{aligned}E_m\varepsilon_{E_m}(t)=E_l\varepsilon_{E_l}(t)(1-P(\varepsilon_{E_l}(t)))+E_l\int_0^{\varepsilon_{E_l}(t)}\varepsilon_b p(\varepsilon_b)d\varepsilon_b\\ +\eta_{m_u}\varepsilon'_{\eta_m}(t)(1-P(\varepsilon_{\eta_m(t)}))+\eta_{m_b}\varepsilon'_{\eta_m}(t)P(\varepsilon_{\eta_m(t)}).\end{aligned} \tag{8}$$

Moreover, since $\varepsilon_{E_l}(t)=\varepsilon_{\eta_m}(t)=\varepsilon(t)-\varepsilon_{E_m}(t)$ from Eq. (2) and, hence, $\varepsilon'_{E_l}(t)=\varepsilon'_{\eta_m}(t)=\varepsilon'(t)-\varepsilon'_{E_m}(t)$, Eq. (8) can be rewritten as

$$\varepsilon'_{E_m}(t)=\varepsilon'(t)+\frac{\frac{E}{\alpha}(e^{-\alpha(\varepsilon(t)-\varepsilon_{E_m}(t))}-1)-\varepsilon_{E_m}(t)}{A(\tau_{m_u},\tau_{m_b},\varepsilon_{E_m}(t),\varepsilon(t),\alpha)}, \tag{9}$$

where $E=E_l/E_m$ is the ratio between the elastic moduli of the crosslinks and the microfibrils. In Eq. (9), for ease of writing, $A=A(\tau_{m_u},\tau_{m_b},\varepsilon_{E_m}(t),\varepsilon(t),\alpha)$ is set to be

$$A(\tau_{m_u},\tau_{m_b},\varepsilon_{E_m}(t),\varepsilon(t),\alpha)=\tau_{m_b}+(\tau_{m_u}-\tau_{m_b})e^{-\alpha(\varepsilon(t)-\varepsilon_{E_m}(t))}, \tag{10}$$

where $\tau_{m_u}=\eta_{m_u}/E_m$ and $\tau_{m_b}=\eta_{m_b}/E_m$ are called relaxation times. The relaxation time is the amount of time that is needed to the stress to decrease and become steady when the strain is fixed to a constant value.

By recalling Eqs. (1) and (3), the total stress of a collagen fiber can be written as

$$\sigma(t)=E_m\varepsilon_{E_m}(t). \tag{11}$$

After differentiating both sides of Eq. (11) with respect to t, one obtains that

$$\sigma'(t)=E_m\varepsilon'_{E_m}(t). \tag{12}$$

Eqs. (9) and (12) form a system of ordinary differential equations that, with appropriate initial conditions, can be solved to describe the mechanical behavior of a collagen fiber.

3.3. Total stress of a collagen fiber

In order to describe the total (elastic and viscous) stress–strain curve of a collagen fiber as computed from incremental stress relaxation tests, the system of ordinary differential equations given by Eqs. (9) and (12) can be solved by assuming that the strain of the collagen fiber, $\varepsilon(t)$, has the form

$$\varepsilon(t)=at, \tag{13}$$

where $t>0$ and a is a constant representing the strain rate. It must be noted that, during incremental stress relaxation tests, the strain rate used to strain the collagen fiber to different increasing levels of strain does not change and is constant.

3.4. Elastic stress of a collagen fiber

The elastic stress–strain curve of a collagen fiber is assumed to be determined only by its constituent microfibrils and their crosslinks. The contribution of the interfibrillar matrix represented by the viscous dashpots in Fig. 2 is neglected. Thus, the collagen fiber is modeled as shown schematically in Fig. 3.

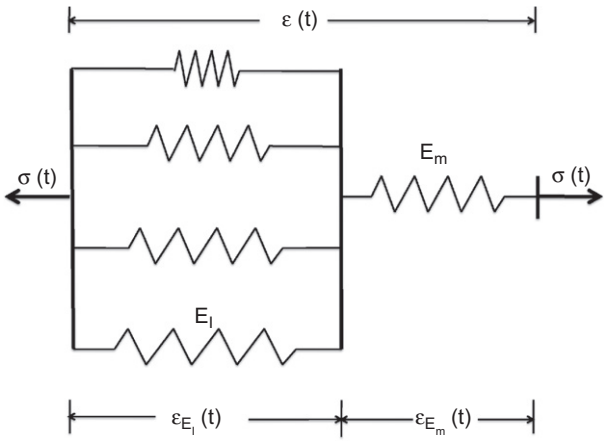

Fig. 3. Schematic of the elastic model.

The elastic stress of a collagen fiber, $\sigma_e(t)$, is then given by

$$\sigma_e(t)=\sigma_{E_m}(t)=\sigma_{E_l}(t), \tag{14}$$

while the elastic strain of the collagen fiber, $\varepsilon_e(t)$, is given by

$$\varepsilon_e(t)=\varepsilon_{E_m}(t)+\varepsilon_{E_l}(t). \tag{15}$$

From Eqs. (3) and (4), one observes that Eq. (14) can be rewritten as

$$E_m\varepsilon_{E_m}(t)=E_l\varepsilon_{E_l}(t)(1-P(\varepsilon_{E_l}(t)))+E_l\int_0^{\varepsilon_{E_l}(t)}\varepsilon_b p(\varepsilon_b)\,d\varepsilon_b. \tag{16}$$

By differentiating both sides of Eq. (16) with respect to ε_e and suppressing the time dependency, one has that

$$\frac{d\varepsilon_{E_m}}{d\varepsilon_e}=\frac{E_l}{E_m}e^{-\alpha\varepsilon_{E_l}}\frac{d\varepsilon_{E_l}}{d\varepsilon_e}. \tag{17}$$

By recalling that $\varepsilon_{E_l}=\varepsilon_e-\varepsilon_{E_m}$ from Eq. (15), Eq. (17) can be written as

$$\frac{d\varepsilon_{E_m}}{d\varepsilon_e}=\frac{E}{e^{\alpha(\varepsilon_e-\varepsilon_{E_m})}+E}, \tag{18}$$

where, as before, $E=E_l/E_m$. From Eqs. (3) and (14), it follows that the elastic stress of a crosslinked collagen fiber is

$$\sigma_e=E_m\varepsilon_{E_m}. \tag{19}$$

By differentiating Eq. (19) with respect to ε_e, one obtains that

$$\frac{d\sigma_e}{d\varepsilon_e}=E_m\frac{d\varepsilon_{E_m}}{d\varepsilon_e}. \tag{20}$$

The system of ordinary differential equations formed by Eqs. (18) and (20) with appropriate initial conditions can be used to compute the elastic stress–strain relationship for a collagen fiber.

3.5. Stress relaxation of a collagen fiber

The stress relaxation of the collagen fiber can be determined by solving the system of ordinary differential equations formed by Eqs. (9) and (12). The strain history of the collagen fiber, $\varepsilon(t)$, is assumed to have the form

$$\varepsilon(t)=\begin{cases}at & \text{for } 0\le t<t_0,\\ \varepsilon_0 & \text{for } t\ge t_0,\end{cases} \tag{21}$$

where a and t_0 are constants $at_0=\varepsilon(t_0^-)=\varepsilon(t_0^+)=\varepsilon_0$. Specifically, the constant a represents the strain rate used to increase the strain from zero to a constant value, ε_0, which is maintained during stress relaxation starting at a time t_0.

For $0 \le t < t_0$, $\varepsilon'(t) = a$. By imposing the initial condition $\sigma(0) = 0$ and noting that $\varepsilon_{E_m}(0) = 0$, the system of ordinary differential equations, Eqs. (9) and (12), can be solved to determine $\sigma(t_0)$ and $\varepsilon_{E_m}(t_0)$, which are then used as initial conditions when solving the system of differential equations for $t > t_0$. For $t > t_0$, $\varepsilon(t) = \varepsilon_0$ and $\varepsilon'(t) = 0$ and by imposing the previously determined initial conditions on $\sigma(t_0)$ and $\varepsilon_{E_m}(t_0)$ the system of ordinary differential equation can be solved to compute the stress $\sigma(t)$, which defines the stress relaxation of the collagen fiber.

4. Results

4.1. Experimental results

Incremental stress relaxation tests were performed at strain levels of 2.4%, 4.8%, 7.3%, 9.7% and 12.1% on a total of 14 reconstituted collagen fibers of rat tail tendons. The peak stresses at different strain levels during each relaxation test were used to generate the total stress–strain data while the equilibrium stresses were used to create the elastic stress–strain data. The average values of the elastic stress–strain, total stress–strain and stress relaxation data at different strain levels were computed and plotted with their standard deviations in Figs. 4–10. A single outlier Grubbs' test was used to detect statistical outliers (specimens) that were skewing the standard deviations. However, the test confirmed that there were no outliers.

4.2. Parameter estimation

There were four parameters, $\{E, \alpha, \tau_{m_u}, \tau_{m_b}\}$, in the proposed modeling framework that needed to be estimated by using experimental data to describe the mechanical behavior of a collagen fiber. The elastic constant of the microfibrils, E_m, was set equal to 12 GPa as suggested by preliminary molecular dynamics studies carried out by the authors. The values of the parameters were determined uniquely by using the experimental

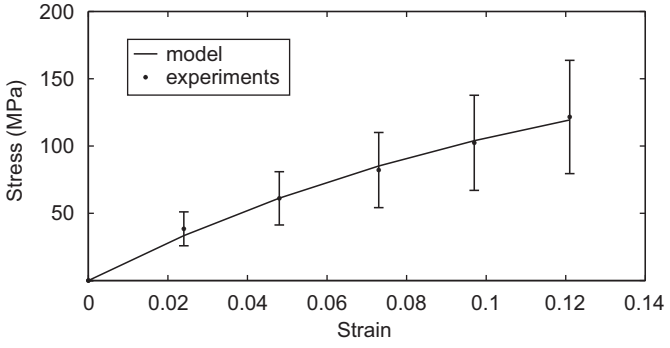

Fig. 4. Experimental elastic stress–strain curve of reconstituted collagen fibers of rat tail tendons and model fit with $E = 0.14$ and $\alpha = 9.4$ ($R^2 = 0.99$).

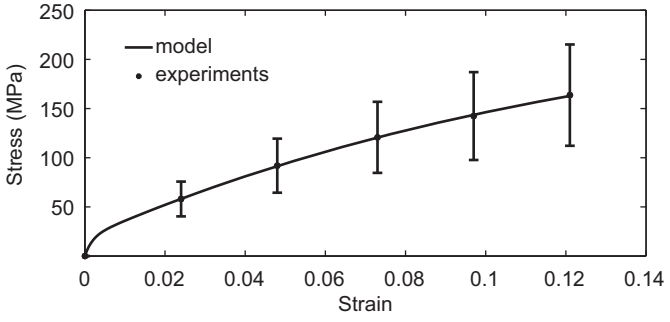

Fig. 5. Experimental total stress–strain curve of reconstituted collagen fibers of rat tail tendon and model fit with $\tau_{mu} = 1.2$ s and $\tau_{mb} = 3.0$ s ($R^2 = 0.99$). Note that $E = 0.14$ and $\alpha = 9.4$.

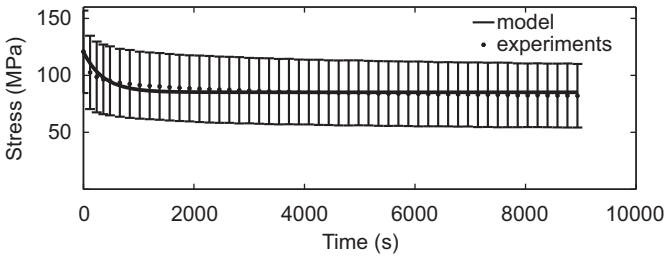

Fig. 6. Experimental stress relaxation data collected at 7.3% strain from reconstituted collagen fibers of rat tail tendon and model fit with $\tau_{mb} = 851$ s ($R^2 = 0.8467$). Note that $E = 0.14$, $\alpha = 9.4$ and $\tau_{mu} = 1.2$ s.

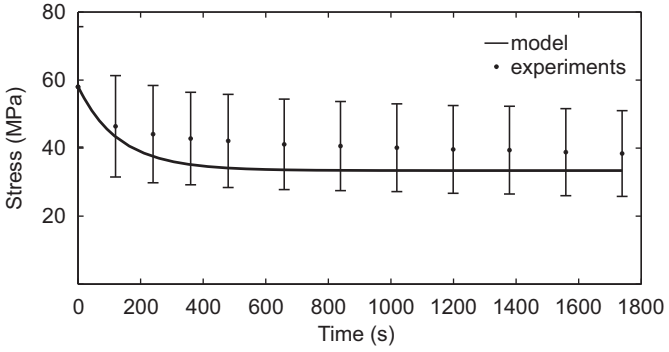

Fig. 7. Stress relaxation at 2.4% strain: experimental data collected from reconstituted collagen fibers of rat tail tendon and model prediction.

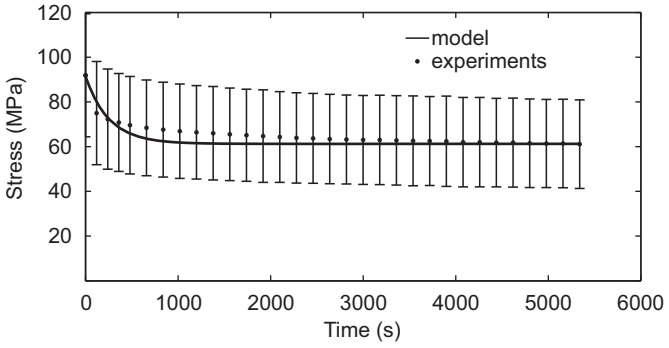

Fig. 8. Stress relaxation at 4.8% strain: experimental data collected from reconstituted collagen fibers of rat tail tendon and model prediction.

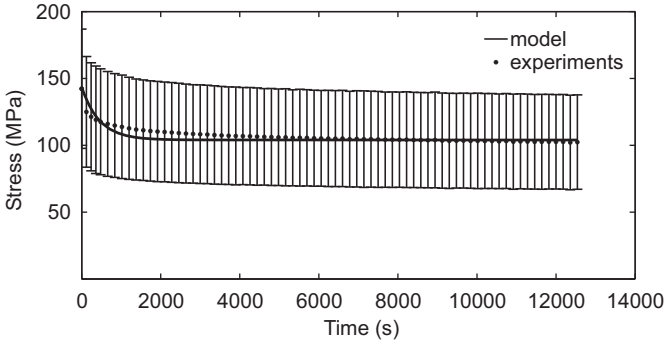

Fig. 9. Stress relaxation at 9.7% strain: experimental data collected from reconstituted collagen fibers of rat tail tendon and model prediction.

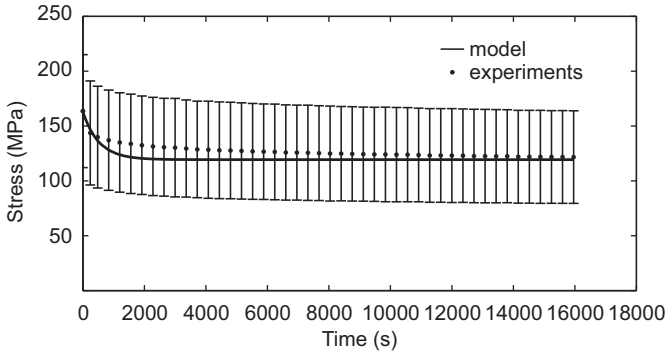

Fig. 10. Stress relaxation at 12.1% strain: experimental data collected from reconstituted collagen fibers of rat tail tendon and model prediction.

data and implementing the nonlinear least squares method in Matlab (the MathWorks, Inc.). The first set of parameters, E and α, which determine the elastic response of the collagen fiber, were found by curve fitting the system of ordinary differential equations, Eqs. (18) and (20), to the average elastic stress–strain data. The results of the fitting and the experimental data are shown in Fig. 4. It was found that $E=0.14$ and $\alpha=9.4$ provided the best fit with $R^2=0.99$.

During incremental stress-relaxation tests, each collagen fiber was strained to different strain levels using the same strain rate, $\varepsilon'=0.16\%\ s^{-1}$. Therefore, in order to fit the average of the total strain–stress curves by using the system of ordinary differential equations formed by Eqs. (9) and (12), it was assumed that $a=0.16\%\ s^{-1}$ in Eq. (13). After setting $E=0.14$ and $\alpha=9.4$, the parameters τ_{m_u} and τ_{m_b} were determined to be 1.2 s and 3.0 s, respectively. The results of the fitting are presented in Fig. 5 where $R^2=0.99$.

The values of the parameters τ_{m_u} and τ_{m_b} could not be computed uniquely by fitting the average stress relaxation data. Thus, τ_{m_u} was fixed to the value determined by fitting the average total stress–strain data in order to uniquely determine τ_{m_b} from the average stress relaxation data at one strain level and *predict* the stress relaxation at different strain levels. The average stress relaxation data recorded by subjecting the collagen fibers to a constant strain of 7.3% was thus used to compute the value of τ_{m_b} in the model represented by Eqs. (9) and (12) while the other parameters, $\{E,\alpha,\tau_{m_b}\}$, were fixed to the values computed by fitting the elastic and total stress–strain data. The value of the constant a was set to be $0.16\%\ s^{-1}$ in Eq. (21), which is used to determine the initial conditions for the system of differential equations given by Eqs. (9) and (12). The value of τ_{m_b} that provided the best fit was found to be 851 s. The results of the fitting are shown in Fig. 6 ($R^2=0.8467$).

The values of the parameters, $\{E,\alpha,\tau_{m_u}\}$, which were found from fitting the total and elastic stress–strain data and the value of the parameter τ_{m_b}, which was determined from fitting the stress relaxation data collected at 7.3% strain, were then employed to predict stress relaxation of the collagen fibers at different strains: 2.4%, 4.8%, 9.7% and 12.1%. The initial conditions for the system of ordinary differential equations for stress relaxation were computed by using the solution of the system of ordinary differential equations obtained with the total stress–strain data. The comparison between the model predictions for stress relaxation and the experimental data are shown in Figs. 7–10.

4.3. Influence of parameters on model predictions

The role of each model parameter in describing the total and elastic stress–strain behaviors and stress relaxation of collagen fibers was investigated. The predictions of the proposed model were plotted for various values of the parameters. The parameters, which were not varied, were fixed to the values obtained from curve fitting the total and elastic stress–strain and stress relaxation experimental data, namely $E=0.14$, $\alpha=9.4$, $\tau_{m_u}=1.2$ s and $\tau_{m_b}=851$ s. It was observed that as the constant E increased, the stiffness of the collagen fiber significantly increased with strain (Fig. 11). For stress relaxation, one could observe that when E increased, the stress reached a higher equilibrium value in a shorter time (Fig. 16).

The effect of the rate parameter, α, of the exponential probability density function on the total stress–strain behavior is shown in Fig. 12 while the corresponding probability density function is presented in Fig. 13. As α increased, the probability that the crosslinks break became higher for lower values of the strain (Fig. 13) and, consequently, the stress in the total stress–strain curve became lower (Fig. 12). Stress relaxation was also influenced by the value of α: as α increased the value of the equilibrium stress decreased and the time needed to reach such equilibrium stress also increased (Fig. 17).

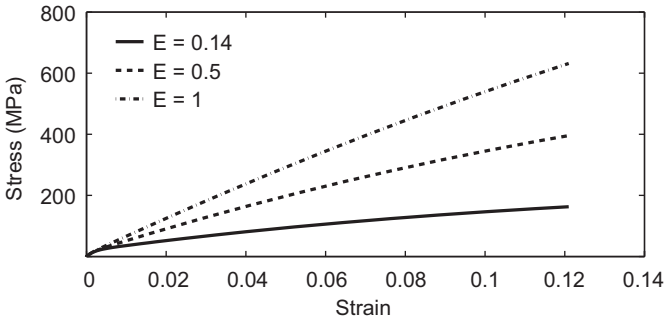

Fig. 11. Influence of the model parameter E on total stress–strain behavior.

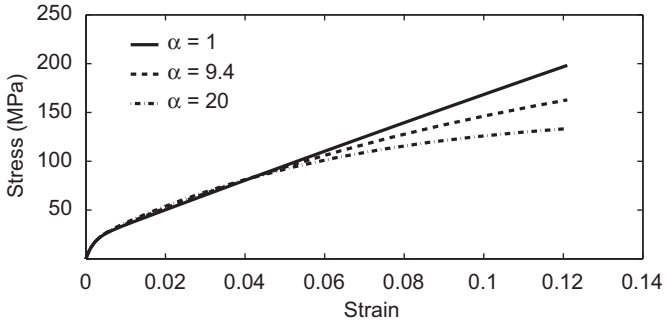

Fig. 12. Influence of the rate parameter α on total stress–strain behavior.

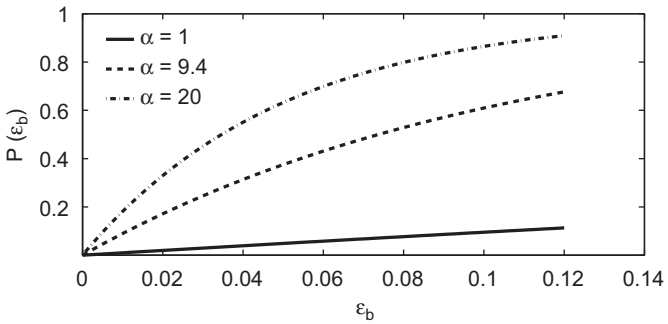

Fig. 13. Influence of the rate parameter α on the exponential cumulative distribution function.

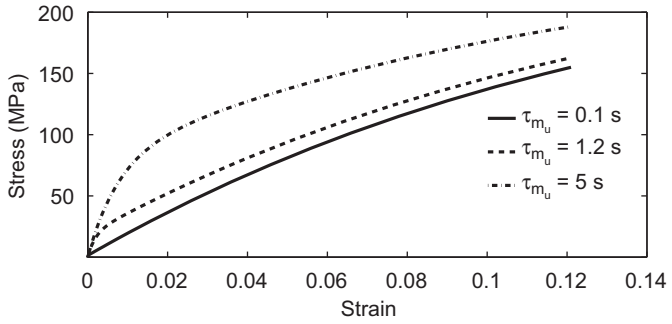

Fig. 14. Influence of the model parameter τ_{m_u} on the total stress–strain behavior.

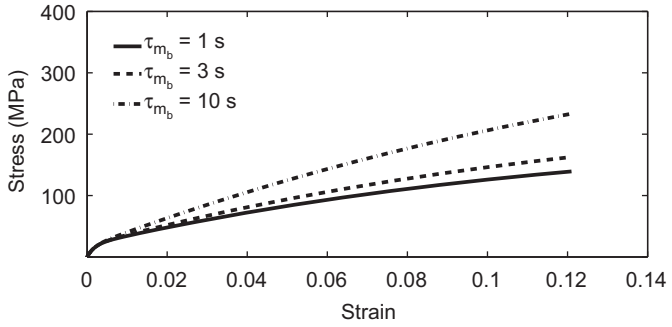

Fig. 15. Influence of the model parameter τ_{m_b} on the total stress–strain behavior.

The relaxation times τ_{m_u} and τ_{m_b} determined the total stress–strain behavior of collagen fibers. As shown in Figs. 14 and 15, the stress increased over strain as τ_{m_u} and τ_{m_b} increased, respectively. It was also observed that, for large value of the strain, the stiffness decreased as τ_{m_u} increased while it increased as τ_{m_b} increased. Finally, the influence of the relaxation times, τ_{m_u} and τ_{m_b}, on the stress relaxation is shown in Figs. 18 and 19, respectively. As τ_{m_u} and τ_{m_b} increased, the stress increased over time and reached the equilibrium state after a longer interval of time.

5. Discussion and conclusions

A new viscoelastic model was presented to describe the elastic and viscoelastic properties of individual collagen fibers determined from incremental stress relaxation tests. The model, for which the schematic is presented in Fig. 2, was formulated by accounting for the mechanical contributions of the microfibrils, the crosslinks among microfibrils and the interfibrillar matrix in a collagen fiber. The progressive failure of crosslinks was assumed to be responsible for the nonlinearities observed in the total and elastic stress–strain curves. The viscous properties of the interfibrillar matrix changed progressively as the crosslinks failed and induced nonlinearities in the total stress–strain and stress relaxation responses. The incremental stress relaxation experiments were conducted on dry collagen fibers reconstituted from rat tail tendons. The total and elastic stress–strain data and the stress relaxation data at different strain levels collected from these experiments were then used to estimate the model parameters and analyze its predictive capabilities.

The parameters in the proposed model were directly related to the composition of a collagen fiber. They were estimated by fitting total stress–strain, elastic stress–strain and stress-relaxation data as shown in Figs. 4–6, respectively. The elastic modulus of the microfibrils, E_m, comprising the collagen fiber was fixed at 12 GPa as estimated by our preliminary molecular dynamics simulations. This estimated value fell within the range of values reported in the literature (Gautieri et al., 2011). The parameters, which were determined from the elastic stress–strain data, were $E=0.14$ and $\alpha=9.4$. The value for the parameter E indicated that the microfibrils were stiffer than the crosslinks in the collagen fiber. The parameter α defined the probability density function that governed the continuous breakage of the crosslinks. Fig. 13 indicated, for example, that at 12% strain, the maximum strain used in the experiments, more than 70% of the crosslinks among microfibrils failed. The total stress–strain data obtained from the incremental stress relaxation tests were used to estimate the other two model parameters, τ_{m_u} and τ_{m_b}, which denoted the relaxation times of the interfibrillar matrix with unbroken and broken crosslinks. The values found for these parameters, $\tau_{m_u}=1.2$ s and $\tau_{m_b}=3.0$ s, suggested that the time for relaxation is longer for the interfibrillar matrix having broken crosslinks.

The predictions of the stress relaxation response at different strain levels, 2.4%, 4.8%, 9.7% and 12.1%, were presented in Figs. 7–10. These predictions were made by using the values of the parameters estimated by fitting the elastic and total stress–strain data and the stress relaxation data collected at 7.3% strain. The stress values predicted by the system of ordinary differential equations fell within the range of values recorded from the experiments. However, there was a common trend in the predictions that appeared to be in contrast with the experimental observations: the stress reached equilibrium values earlier in time.

The influence of each model parameter on the predictions of total and elastic stress–strain and stress relaxation behaviors were presented in Figs. 11–19. In Fig. 11, the total stress-strain response was shown for different numerical values of E. The parameter E, which represented the ratio between the elastic moduli of the crosslinks and the microfibrils, played a significant role on increasing the stiffness of the collagen fibers. These findings are in agreement with the previous studies in which an increase in crosslinks produced an increase in the stiffness of collagenous tissues (Puxkandl et al., 2002; Hansen et al., 2009). The parameter E also determined the values of

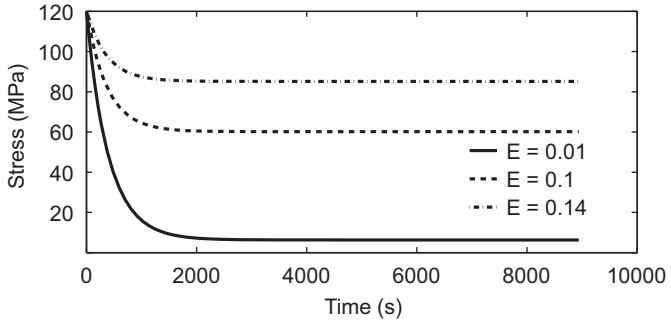

Fig. 16. Influence of the model parameter E on stress relaxation.

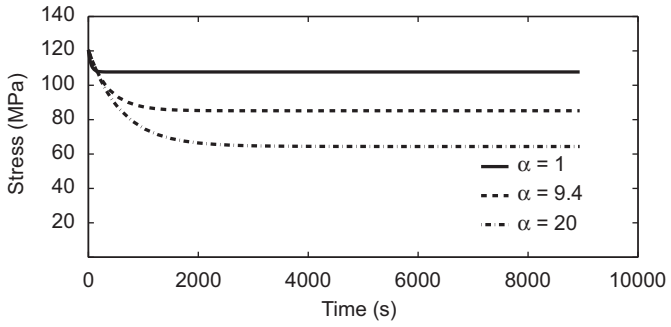

Fig. 17. Influence of the rate parameter α on stress relaxation.

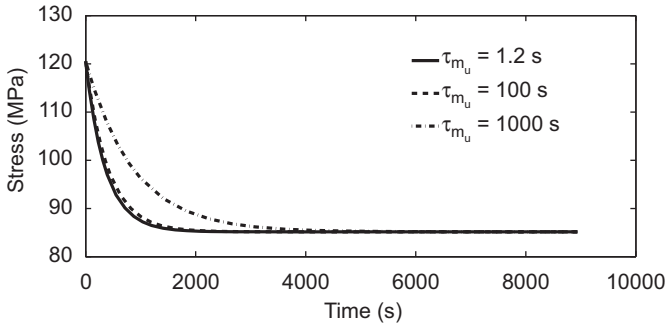

Fig. 18. Influence of the model parameter τ_{m_u} on stress relaxation.

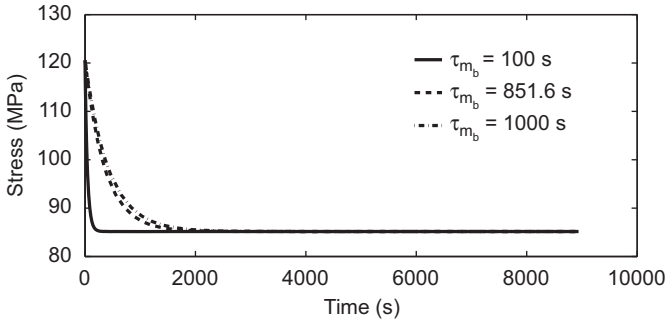

Fig. 19. Influence of the model parameter τ_{m_b} on stress relaxation.

the equilibrium stress during stress relaxation (Fig. 16). Indeed, as E increased, the values of the equilibrium stress increased while the values of the relaxation time decreased. These results indicated that the collagen fiber relaxed faster during relaxation when it had more crosslinks as observed in recently published experimental studies (Usha et al., 2001).

In Fig. 12 the total stress–strain curve of the collagen fiber was reported for different values of the rate parameter, α, of the exponential probability density function that defined the continuous failure of crosslinks while in Fig. 13 the corresponding cumulative density function was presented. As α increased, the percentage of crosslinks that failed also increased, especially at large strains (Fig. 13) and, hence, the total stress of the collagen fiber decreased at these strains (Fig. 12). This continuous mechanism of progressive failure of the crosslinks in the collagen fiber is similar to the one proposed by other investigators for modeling the breakage of elastic fibers in bundles (Raischel et al., 2006; Guo and De Vita, 2009). In this study, the parameter α also contributed to define the stress relaxation in collagen fibers as illustrated in Fig. 17. The stress relaxation was more pronounced for collagen fibers having a higher percentage of broken crosslinks for which α had greater values (Fig. 13).

The total stress–strain curve of each collagen fiber computed from incremental stress relaxation tests was found to be almost bilinear (Fig. 5). A bilinear behavior was also reported by other researchers who investigated the mechanical properties of dry collagen fibers (Kato et al., 1989). However, the paucity of data in the initial region of the stress–strain curve and the presence of relevant error bars in the data do not allow to exclude that the observed behavior could be simply linear. One could observe from Fig. 14 that in a collagen fiber the stress over strain increased with τ_{m_u}, while the stiffness increased for small values of the strain and, although only slightly, decreased for large values of the strain. Unlike τ_{m_u}, the stress over small values of the strain remained almost unchanged while it increased for large values of the strain when τ_{m_b} increased. Consequently, the stiffness of the collagen fiber for small values of the strain remained unchanged while it increased for large values of the strain. These parametric studies indicated that the viscous properties of the interfibrillar matrix with unbroken crosslinks had a significant role on the total stress of the collagen fiber at small strain while the viscous property of the interfibrillar matrix with broken crosslinks had a significant role on the total stress at large strain.

The relaxation times τ_{m_u} and τ_{m_b} also influenced the stress relaxation as illustrated in Figs. 18 and 19, respectively. It was clearly shown that when the relaxation times had greater values, the stress of the collagen fiber reached equilibrium after a longer interval of time while the value of the stress at equilibrium was unaffected. Two different relaxation times, a fast relaxation time and a slow relaxation time, were also observed in experimental studies on rat tail tendon collagen fibers conducted by other investigators (Usha et al., 2001; Gupta et al., 2010).

One limitation of this study is that the values of the four model parameters $E=0.14$, $\alpha=9.9$, $\tau_{m_u}=1.2$ s, and $\tau_{m_b}=3.0$ s, which were fitted to the average elastic and total stress–strain data, were unable to *predict* the stress relaxation data. This was, perhaps, due to the different viscoelastic responses described by the average total stress–strain data and the average stress relaxation data in incremental stress relaxation tests. For this reason, τ_{m_u} and τ_{m_b} were fitted to stress relaxation data collected at one strain level. Because the results of this curve fitting did not produce a unique set of values for τ_{m_u} and τ_{m_b}, the value of τ_{m_u} was kept to the value computed by curve fitting the average total stress–strain data. Thus, τ_{m_u} was fixed to 1.2 s to determine uniquely a new value for τ_{m_b}. It must be noted that τ_{m_u} was fixed to the value computed by fitting the average total stress–strain data because it was assumed that this value was more accurate than the value of τ_{m_b} computed using the same data. According to the parametric analysis, τ_{m_u} appeared to determine the initial portion of the total stress–strain curve (Fig. 14) while τ_{m_b} appeared to define the final portion of such curve (Fig. 15). Moreover, the stress–strain data computed from incremental stress relaxation tests represented more closely the total (elastic and viscoelastic) behavior of the collagen fiber in their initial portion than in their final portion. Indeed, in incremental stress relaxation tests, the total stress–strain curve was computed from the peak stresses at different strain levels during each relaxation test. As the number of consecutive stress relaxation tests increased, the viscous contributions to the total stress–strain data decreased due to repetitive tests. Hence, given the influence of τ_{m_u} on the initial region of the total stress–strain curve and the higher fidelity of the initial portion of the total stress–strain data, it was considered more appropriate to fix τ_{m_u} (and not τ_{m_b}) to the value determined by fitting the average total stress–strain data.

The reconstituted collagen fibers from rat tail tendons were subjected to incremental stress relaxation tests in ambient room air (relatively dry). Therefore, the total and elastic stresses were much greater than those reported for their hydrated counterparts (Silver et al., 2000). Interestingly, the incremental stress-relaxation data resembled those of hydrated native rat tail tendons, aged to similar extents. This implies that the mechanism that imparts native rat tail tendon with its viscoelastic properties was strengthened in the less hydrated state (ambient air). In native rat tail tendon, the collagen type I microfibrils interact with microfibril-associated collagens, proteoglycans, and water; however, in reconstituted collagen type I fibers, microfibrils are lacking many of these supporting macromolecules that facilitate interaction between microfibrils (i.e., microfibril organization and microfibril slippage). These differences would contribute to the drastic differences in the viscoelastic response of native and reconstituted rat tail tendon collagen fibers tested in the hydrated state (Silver et al., 2001a). In this case, drying most likely

led to a departure of water from the interfibrillar and inter-molecular spaces, leading to a denser arrangement of collagen microfibrils and molecules (i.e., increased volume fraction of polymer). This in-turn would be expected to produce an increased axial ratio and effective fibril length, thereby accounting for the increases in the total and elastic stress (Silver et al., 2001a). Fibril length and diameter are expected to influence the strength and stiffness at the level of the collagen fiber. Indeed, Silver et al. (2001a) found that effective fibril length was strongly correlated to ultimate tensile strength and elastic modulus. Fiber diameter was also correlated with ultimate tensile strength, but the correlation was not as strong as the one between effective fibril length and ultimate tensile strength.

Each incremental stress relaxation test conducted in this study required several hours to be completed. For this reason, the age and extent of crosslinking of the tested collagen fibers were different. Moreover, the collagen fibers were tested over long periods of time in ambient air with different levels of humidity and were not kept hydrated. This was done because the low forces (and stresses) required to test hydrated collagen fibers caused high signal-to-noise ratio in the tensile testing system employed in this study. The differences in the age and extent of crosslinking of the collagen fibers and ambient air humidity are likely responsible for the high variability observed in the mechanical experimental data.

In conclusion, a new modeling framework was presented for describing the mechanical response of collagen fibers exhibited during incremental stress relaxation tests. The modeling approach adopted here could be extended to describe other viscoelastic phenomena in collagen fibers such as, for example, creep and could be also applied to describe the viscoelasticity of other collagenous tissues. More importantly, it could be employed to illustrate the role of crosslink density on the mechanical behavior of collagenous fibers and tissues. It is likely that the viscoelastic behavior of collagen fibers depends also on their fibrillar structure, fascicle size, water binding properties and the nature of the interfibrillar matrix. Therefore, future experimental and theoretical studies will need to be carried out to uncover the role of the ultrastructure of collagen fibers on their viscoelasticity.

Acknowledgment

This material is based upon work supported by the National Science Foundation under Grant no. 0932024. The authors thank Dr. Joseph Orgel from the Illinois Institute of Technology in Chicago for useful discussions about the role and content of proteoglycans in type I collagen fibers.

References

Avery, N., Bailey, A., 2008. Restraining cross-links responsible for the mechanical properties of collagen fibers: natural and artificial. Collagen, 81–110.
Couppe, C., Hansen, P., Kongsgaard, M., Kovanen, V., Suetta, C., Aagaard, P., 2009. Mechanical properties and collagen cross-linking of the patellar tendon in old and young men. J. Appl. Physiol. 107, 880–886.
Davison, P.F., Brennan, M., 1983. The organization of crosslinking in collagen fibrils. Connect. Tissue Res. 11, 135–151.
De Tommasi, D., Puglisi, G., Saccomandi, G., 2006. A micromechanics-based model for the Mullins effect. J. Rheol. 50, 495.
Deyl, Z., Adam, M., 1989. Separation methods for the study of collagen and treatment of collagen disorders. J. Chromatogr. 448, 161–197.
Eyre, D.R., Wu, J.J., 2005. Collagen cross-links. Collagen, 207–229.
Gautieri, A., Vesentini, S., Redaelli, A., Buehler, M., 2011. Hierarchical nanomechanics of collagen microfibrils. Nano Lett. 11, 757–766.
Guo, Z., De Vita, R., 2009. Probabilistic constitutive law for damage in ligaments. Med. Eng. Phys. 31, 1104–1109.
Gupta, H.S., Seto, J., Krauss, S., Boesecke, P., Screen, H.R.C., 2010. In situ multi-level analysis of viscoelastic deformation mechanisms in tendon collagen. J. Struct. Biol. 169, 183–191.
Hansen, P., Hassenkam, T., Svensson, R.B., Aagaard, P., Trappe, T., Haraldsson, B.T., Kjaer, M., Magnusson, P., 2009. Glutaraldehyde cross-linking of tendon: mechanical effects at level of the tendon fascicle and fibril. Connect. Tissue Res. 50, 211–222.
Kato, Y.P., Christiansen, D.L., Hahn, R.A., Shieh, S.-J., Goldstein, J.D., Silver, F.H., 1989. Mechanical properties of collagen fibres: a comparison of reconstituted and rat tail tendon fibres. Biomaterials 10, 38–42.
Pins, G.D., Christiansen, D.L., Patel, R., Silver, F.H., 1997. Self-assembly of collagen fibers. Influence of fibrillar alignment and decorin on mechanical properties. Biophys. J. 73, 2164–2172.
Puxkandl, R., Zizak, I., Paris, O., Keckes, J., Tesch, W., Bernstorff, S., Purslow, P., Fratzl, P., 2002. Viscoelastic properties of collagen: synchrotron radiation investigations and structural model. Philos. Trans. R. Soc. 357, 191–197.
Raischel, F., Kun, F., Herrmann, H., 2006. Failure process of a bundle of plastic fibers. Phys. Rev. E 73 (6), 66101.
Raspanti, M., Congiu, T., Guizzardi, S., 2002. Structural aspects of the extracellular matrix of the tendon: an atomic force and scanning electron microscopy study. Arch. Histol. Cytol. 65, 37–43.
Robins, S.P., 1982. Analysis of the crosslinking components in collagen and elastin. Methods Biochem. Anal. 28, 330–379.
Saito, M., Marumo, K., Fujii, K., Ishioka, N., 1997. Single-column high-performance liquid chromatographic-fluorescence detection of immature, mature, and senescent cross-links of collagen. Anal. Biochem. 253, 26–32.
Silver, F., Christiansen, D., Snowhill, P., Chen, Y., 2000. Role of storage on changes in the mechanical properties of tendon and self-assembled collagen fibers. Connect. Tissue Res. 41, 155–164.
Silver, F., Christiansen, D., Snowhill, P., Chen, Y., 2001a. Transition from viscous to elastic-based dependency of mechanical properties of self-assembled type I collagen fibers. J. Appl. Polym. Sci. 79, 134–142.
Silver, F., Ebrahimi, A., Snowhill, P., 2002. Viscoelastic properties of self-assembled type I collagen fibers: molecular basis of elastic and viscous behaviors. Connect. Tissue Res. 43, 569–580.
Silver, F., Freeman, J., DeVore, D., 2001b. Viscoelastic properties of human skin and processed dermis. Skin Res. Technol. 7, 18–23.
Silver, F.H., Freeman, J.W., Seehra, G.P., 2003. Collagen self assembly and the development of tendon mechanical properties. J. Biomech. 36, 1529–1553.
Sims, T., Bailey, A.J., 1992. Quantitative analysis of collagen and elastin cross-links using a single-column system. J. Chromatogr. Biomed. Appl. 582, 49–55.
Usha, R., Subramanian, V., Ramasami, T., 2001. Role of secondary structure on the stress relaxation processes on rat tail tendon (RTT) collagen fibre. Macromol. Biosci. 1, 100–107.